JOURNAL OF SOLID STATE CHEMISTRY 114, 481–485 (1995)

A Molybdenum (V) Diphosphate with a Tunnel Structure: β-$K_2Mo_2O_4P_2O_7$

A. Guesdon, A. Leclaire, M. M. Borel, A. Grandin, and B. Raveau

Laboratoire CRISMAT, CNRS URA 1318, ISMRA, Université de Caen Boulevard du Maréchal Juin, 14050 Caen Cedex, France

Received February 18, 1994; in revised form May 26, 1994; accepted May 27, 1994

A new Mo(V) diphosphate with a tunnel structure, β-$K_2Mo_2O_4P_2O_7$, has been synthesized. This phase can be considered as a low temperature form of the monophosphate α-$K_2Mo_2O_3(PO_4)_2$. It crystallizes in the space group *Pbcn* with a = 9.314(1) Å, b = 8.868(1) Å, c = 10.954(2) Å. The $[Mo_2P_2O_{11}]_\infty$ framework consists of corner-sharing bioctahedral Mo_2O_{10} units and eclipsed P_2O_7 groups. It can be described as the assemblage of two enantiomorphic $[Mo_2P_2O_{12}]_\infty$ layers parallel to (010), themselves built up of $[Mo_2P_2O_{15}]_\infty$ chains, running along c. In these chains one Mo_2O_{10} unit alternates with one P_2O_7 group along c. Each Mo_2O_{10} unit of two edge-sharing octahedra has two free apices, leading to the classical geometry of the Mo(V) octahedra characterized by an abnormally short Mo–O bond. The framework delimits tunnels running along b, where the potassium ions are located with a tricapped trigonal prismatic coordination.

INTRODUCTION

A large number of pentavalent molybdenum phosphates have been synthesized in the past 10 years (for a review see Ref. (1)). The variety of structures are the result of the high flexibility introduced by the molybdenyl ions that impose a free apex for the MoO_6 octahedra. Consequently, polymorphism is one characteristic of these compounds, as shown for instance for the phosphates $KMo_2P_3O_{13}$ that exhibit several different forms according to the experimental conditions of synthesis (2–4). However, very few Mo(V) diphosphates have been discovered to date in spite in the highly flexible character of Mo(V). Only four pure Mo(V) diphosphates, $KMoP_2O_8$ (5), $CsMoP_2O_8$ (6), $BaMo_2P_4O_{16}$ (7), and $AgMo_2P_8O_{33}$ (8), have been isolated, whereas in the phosphates $AMo_2P_3O_{13}$, monophosphate, and diphosphate groups coexist (1). Taking into consideration the dramatic influence of the experimental conditions of synthesis and especially of temperature upon the structure of these phases we have reinvestigated the K–Mo(V)–P–O system. The present paper deals with the synthesis and crystal structure of a new diphosphate, called β-$K_2Mo_2O_4P_2O_7$, that exhibits a very different structure from the first form, α-$K_2Mo_2O_3(PO_4)_2$, which is a monophosphate (9).

EXPERIMENTAL

The compounds K_2CO_3, $H(NH_4)_2PO_4$, and MoO_3 are first mixed in adequate proportions in order to realize the final phase $K_2Mo_2O_4P_2O_7$. The mixture is first heated in air at 673 K in order to eliminate CO_2, H_2O, and NH_3. In a second step the resulting finely ground product is mixed with the appropriate amount of molybdenum and sealed in an evacuated silica ampoule. This sample is then heated to 973 K for 2 days and cooled at 2 K per h to 773 K. The sample is finally quenched to room temperature. Under these conditions, one obtains a brown powder that contains amber crystals. Some of these crystals have been extracted for the single crystal X-ray diffraction study. Their microprobe analysis shows that their composition is identical to that of the brown-red crystals of the previously reported α-form $K_2Mo_2O_3(PO_4)_2$ (9) prepared at 1073 K. However, their cell parameters do not agree with those of the α-form. The powder X-ray pattern was indexed in an orthorhombic cell (Table 1) in agreement with the parameters obtained from the single crystal study.

STRUCTURE DETERMINATION

An amber crystal with dimensions 0.051 × 0.051 × 0.026 mm was selected for the structure determination. The cell parameters were determined and refined by diffractometric techniques at 294 K with a least-squares refinement based upon 25 reflections with $18° < \theta < 25°$ (Table 2). The data were collected on a CAD4 Enraf-Nonius diffractometer with the data collection parameters given in Table 2. The reflections were corrected for Lorentz, polarization, absorption, and secondary extinction effects.

The structure was solved by the heavy atom method with the space group *Pbcn* (No. 60), in agreement with the observed extinctions: $h + k = 2n + 1$ for $hk0$, $k = 2n + 1$ for $0kl$, and $l = 2n + 1$ for $h0l$. The refinement

0022-4596/95 $6.00

TABLE 1
Interreticular Distances

hkl	d_{calc} (Å)	d_{obs} (Å)	I (%)	hkl	d_{calc} (Å)	d_{obs} (Å)	I (%)
110	6.422	6.415	14	204	2.361	2.361	1
111	5.540	5.532	100	024	2.330	2.329	6
102	4.721	4.718	36	400	2.328		
200	4.657	4.655	22	322	2.307	2.305	7
020	4.434	4.432	68	313	2.285	2.281	1
112	4.167	4.168	1	214	2.281		
211	3.859	3.857	14	124	2.260	2.256	1
202	3.548	3.546	10	040	2.217	2.217	41
022	3.446	3.448	15	411	2.206	2.204	16
212	3.294	3.294	23	041	2.173	2.171	4
122	3.232	3.232	92	402	2.143	2.143	4
220	3.211	3.210	97	330	2.141		
221	3.082	3.082	5	141	2.116	2.112	1
310	2.930	2.930	5	323	2.087	2.083	9
023	2.819	2.815	33	224	2.084		
130	2.817			412	2.083		
004	2.739	2.738	43	115	2.073	2.072	40
213	2.734			420	2.062	2.060	8
302	2.701	2.699	89	233	2.060		
123	2.698			042	2.055	2.053	8
104	2.627	2.625	7	304	2.054		
312	2.584	2.582	4	421	2.026	2.020	16
321	2.477	2.473	1	240	2.002	1.999	1
231	2.433	2.425	5	314	2.001		
223	2.411	2.407	2	332	1.994		

of the atomic coordinates and their thermal anisotropic factors led to $R = 0.035$ and $R_w = 0.036$ and to the atomic parameters summarized in Table 3.

DESCRIPTION OF THE STRUCTURE AND DISCUSSION

The projection of the structure of this new phase along **b** (Fig. 1) shows that its $[Mo_2P_2O_{11}]_\infty$ framework consists of diphosphate groups sharing their apices with bioctahedral Mo_2O_{10} units. This framework delimits tunnels running along **b**, where the potassium ions are located. Thus, this structure is completely different from that of the isochemical compound $K_2Mo_2O_3(PO_4)_2$ that is characterized by monophosphate groups.

The originality of $K_2Mo_2O_4(P_2O_7)$, with respect to other Mo(V) phosphates deals with the bioctahedral Mo_2O_{10} units that are built up of two edge-sharing MoO_6 octahedra. Such units have been previously observed in molybdenum phosphates by Haushalter *et al.* (10). In this regard, the behavior of Mo(V) in this particular structure is similar to that of V(III). Many V(III) phosphates are indeed characterized by V_2O_{10} units (11–13); for example, the monophosphate $Cd_3V_4(PO_4)_6$ [11] exhibits a similar fish-bone arrangement of the V_2O_{10} units and PO_4 tetrahedra.

The $[Mo_2P_2O_{11}]_\infty$ framework can in fact be described in a very simple manner, as the stacking of two enantiomorphic layers $[Mo_2P_2O_{12}]_\infty$ along **b** (Figs. 2 and 3). These two successive layers are shifted of $c/2$ with respect to each other in such a way that a diphosphate group of one layer shares two apices with a bioctahedral unit of the enantiomorphic adjacent layer (Fig. 2). The geometry of the $[Mo_2P_2O_{12}]_\infty$ layer is characterized by a fish-bone arrangement of the Mo_2O_{10} and P_2O_7 units as shown in Fig. 1. Each layer consists of identical $[Mo_2P_2O_{15}]_\infty$ chains running along **c**, in which one Mo_2O_{10} unit alternates with one P_2O_7 group. Each $[Mo_2P_2O_{15}]_\infty$ chain is linked to an identical chain rotated by 180°, along **a**, the octahedra of one chain sharing one apex with the tetrahedra of the next one. Clearly, the apices of the P_2O_7 groups of two successive chains are pointing up and down respectively (Fig. 1). Note that this arrangement of the polyhedra forms five-sided windows built up from three MoO_6 octahedra and three PO_4 tetrahedra, whose stacking along **b** leads to the tunnels described above (Fig. 1).

From the view of the structure along **a** (Fig. 2) and along **c** (Fig. 3) it appears clearly that the polyhedra form small tunnels running along those directions, so that the K^+ ions are located at the intersection of the [100], [001], and [010] tunnels. Moreover, one observes that each bi-

TABLE 2
Summary of Crystal Data Intensity Measurements and Structure Refinement Parameters for β-$K_2Mo_2O_4P_2O_7$

Crystal data	
Space group	*Pbcn* (No. 60)
Cell dimensions	a = 9.314(1) Å
	b = 8.8679(9) Å
	c = 10.954(2) Å
Volume	904.7(3) Å^3
Z	4
d_{calc}	3.73
Intensity measurements	
λ (Mo$K\alpha$)	0.71073 Å
Scan mode	$\omega - \theta$
Scan width (°)	1.0 + 0.35 tan θ
Slit aperture (mm)	1.03 + tan θ
Max θ (°)	45
Standard reflections	3 (every 3000 sec)
Range	h: 0–18
	k: 0–17
	l: 0–21
Measured reflections	4163
Reflections with $I > 2.5\sigma$	744
μ (mm^{-1})	4.03
Structure solution and refinement	
Parameters refined	79
Agreement factors	R = 0.035, R_w = 0.036
Weighting scheme	Hamilton scheme (See Ref. (16))
Δ/σ max	< 0.04
$\Delta\rho$ (e Å^{-3})	1.18
S	1.007

octahedral Mo_2O_{10} unit exhibits two free apices, both of them directed toward the center of the [001] tunnels (Fig. 3). In fact, the connection between two $[Mo_2P_2O_{12}]_\infty$ layers along **b** can also be described from the assemblage of the $[Mo_2P_2O_{15}]_\infty$ chains running along **c**. One chain out of two belonging to one layer is linked to a similar chain of the

TABLE 3
Positional Parameters and Their Estimated Standard Deviations

Atom	x	y	z	B
K	0.2954(2)	−0.0097(3)	0.4123(2)	1.44(3)
Mo	0.07834(7)	0.23067(7)	0.15380(6)	0.450(6)
P	0.4302(2)	0.3233(2)	0.1273(2)	0.50(3)
O(1)	0.0804(7)	0.4210(6)	0.1377(5)	0.91(9)
O(2)	0.1262(6)	0.2022(7)	0.3234(5)	0.8(1)
O(3)	0.0494(6)	0.2005(8)	−0.0345(5)	1.1(1)
O(4)	0.3005(6)	0.2246(8)	0.1027(5)	0.84(9)
O(5)	0.1080(6)	−0.0144(7)	0.1443(7)	1.3(1)
O(6)	0.5	0.259(1)	0.25	1.1(1)

Note. Anisotropically refined atoms are given in the form of the isotropic equivalent displacement parameter defined as $B = \frac{4}{3}\Sigma_i \Sigma_j \mathbf{a}_i\mathbf{a}_j\beta_{ij}$.

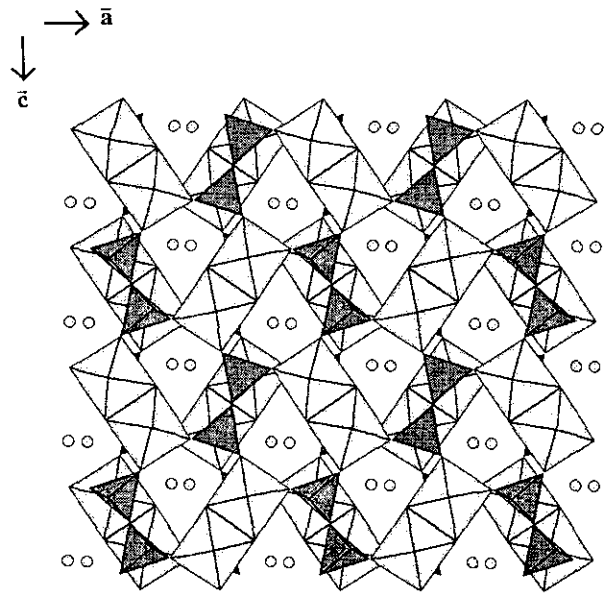

FIG. 1. Projection of β-$K_2Mo_2O_4P_2O_7$ along [010].

enantiomorphic layer in order to form $[Mo_4P_4O_{26}]_\infty$ double chains (Fig. 4), each tetrahedron of one chain sharing one apex with one octahedron of the other chain.

In the $[Mo_2P_2O_{11}]_\infty$ host lattice, each Mo_2O_{10} unit shares six apices with five diphosphate groups; four P_2O_7 groups are located in its basal plane i.e., in the same $[Mo_2P_2O_{12}]_\infty$ layer, and the fifth is linked to the two apical corners of the Mo_2O_{10} unit, i.e., belongs to the adjacent $[Mo_2P_2O_{12}]_\infty$ layer. The MoO_6 octahedron exhibits the characteristic geometry of Mo(V), since it presents one free apex (not shared with other Mo or P) corresponding to a very short Mo–O bond (1.697 Å), the opposite Mo–O bond being the longest one (2.193 Å) (Table 4). The valence calculation (14) confirms the pentavalent character of this molybdenum since a value of 4.94 has been obtained. The Mo–Mo bond (2.564 Å) is similar to that observed in other structures presenting two edge-sharing octahedra.

The diphosphate group is characterized by an eclipsed configuration, with a geometry of the PO_4 tetrahedron similar to that observed in other diphosphates. The P–O distances are characterized by a longer bond (1.597 Å) corresponding to the bridging oxygen O(6) and three shorter P–O bonds (1.49–1.52 Å) (Table 4).

The potassium cation is surrounded by nine oxygen atoms in a tricapped trigonal prism at distances smaller than 3.35 Å. Nevertheless, to obtain a value of 1 using valence calculation (15), only the six nearest oxygens (making the trigonal prism) have to be considered.

CONCLUDING REMARKS

A diphosphate of pentavalent molybdenum with bioctahedral Mo_2O_{10} units has been synthesized for the first

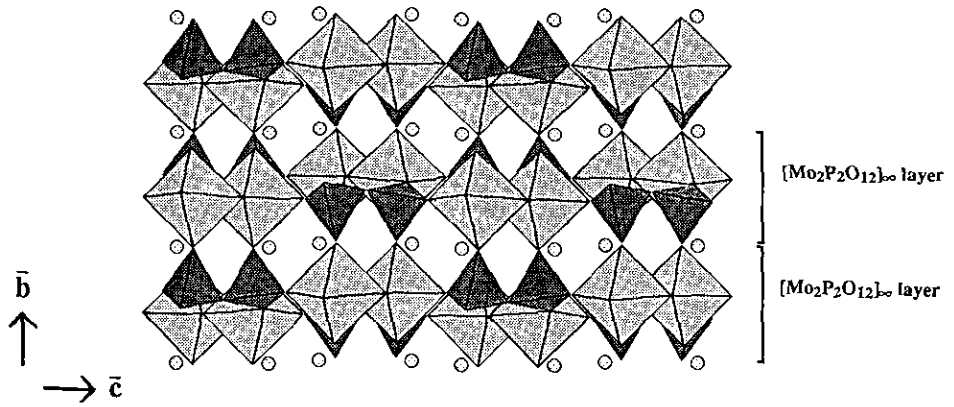

FIG. 2. Projection of β-$K_2Mo_2O_4P_2O_7$ along [100].

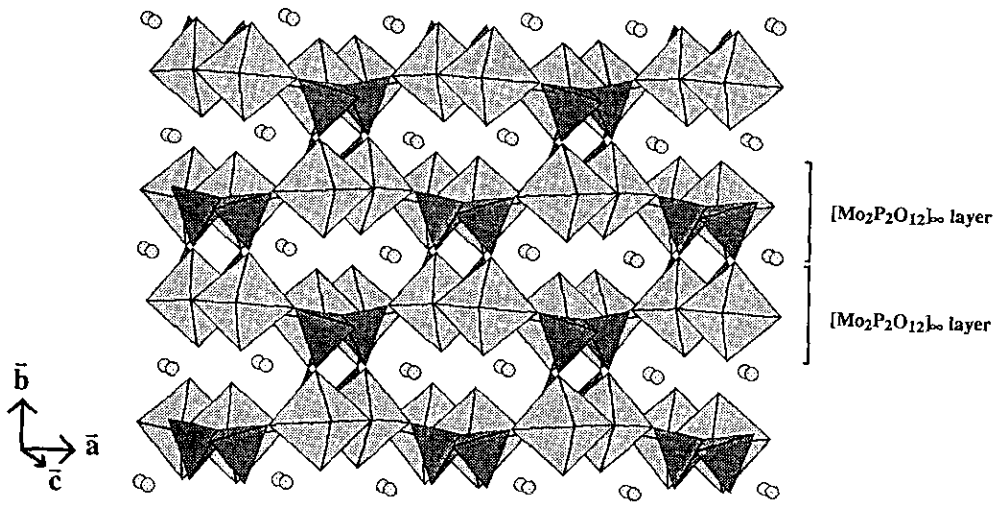

FIG. 3. Assemblage along [010] of $[Mo_2P_2O_{12}]_\infty$ enantiomorphic layers.

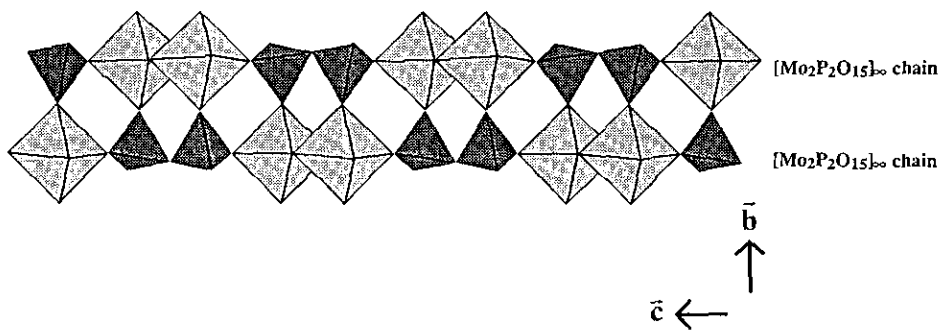

FIG. 4. $[Mo_4P_4O_{26}]_\infty$ double chain.

time. The existence of two very different forms, α-$K_2Mo_2O_3(PO_4)_2$ and β-$K_2Mo_2O_4P_2O_7$, confirms the strong potential of Mo(V) to generate various phosphates, owing to its great flexibility. The very narrow range of temperatures, less than 100 K, that is required to stabilize each of these forms suggests that other forms may exist for the other Mo(V) phosphates prepared up to now. A systematic investigation will be necessary to understand this

chemistry and especially the relative abundance of Mo(V) monophosphates as compared to diphosphates.

TABLE 4
Distances (Å) and Angles (°) in the Polyhedra

Mo	O(1)	O(2)	O(2^{i})	O(3)	O(4)	O(5)
O(1)	1.697(5)	2.844(8)	2.765(9)	2.732(9)	2.718(9)	3.87(1)
O(2)	103.2(3)	1.927(6)	2.85(1)	3.99(1)	2.920(8)	2.751(9)
O(2^{i})	98.9(3)	94.9(2)	1.938(6)	2.832(8)	4.06(1)	2.928(9)
O(3)	91.5(3)	164.0(3)	89.1(2)	2.097(6)	2.788(8)	2.79(1)
O(4)	89.3(3)	91.5(2)	168.2(3)	82.2(2)	2.144(5)	2.814(9)
O(5)	168.3(3)	83.5(3)	90.0(3)	81.0(3)	80.9(3)	2.193(6)

P	O(3)	O(4)	O(5)	O(6)
O(3)	1.520(6)	2.524(8)	2.514(9)	2.432(6)
O(4)	112.5(4)	1.516(7)	2.51(1)	2.480(6)
O(5)	113.1(4)	112.9(4)	1.494(7)	2.53(1)
O(6)	102.5(3)	105.6(4)	109.5(5)	1.597(4)

K–O(2) = 2.638(7) Å
K–O(1^{ii}) = 2.779(8) Å
K–O(4^{v}) = 2.826(7) Å
K–O(2^{iv}) = 2.830(7) Å
K–O(1^{iii}) = 2.839(7) Å
K–O(3^{v}) = 2.908(6) Å
K–O(5^{v}) = 3.091(8) Å
K–O(3^{iii}) = 3.154(7) Å
K–O(1^{iv}) = 3.280(7) Å

Note. Symmetry code: (i) $-x, y, \frac{1}{2} - z$; (ii) $\frac{1}{2} + x, -\frac{1}{2} + y, \frac{1}{2} - z$; (iii) $\frac{1}{2} - x, \frac{1}{2} - y, \frac{1}{2} + z$; (iv) $\frac{1}{2} - x, -\frac{1}{2} + y, z$; and (v) $x, -y, \frac{1}{2} + z$.

REFERENCES

1. G. Costentin, A. Leclaire, M. M. Borel, A. Grandin, and B. Raveau, *Rev. Inorg. Chem.* **13,** 77 (1993).
2. A. Leclaire, J. C. Monier, and B. Raveau, *J. Solid State Chem.* **48,** 147 (1983).
3. A. Leclaire, M. M. Borel, A. Grandin, and B. Raveau, *Acta Crystallogr. Sect. C* **46,** 2009 (1990).
4. A. Leclaire, M. M. Borel, A. Grandin, and B. Raveau, *Z. Kristallogr.* **188,** 77 (1989).
5. C. Gueho, M. M. Borel, A. Grandin, A. Leclaire, and B. Raveau, *Z. Anorg. Allg. Chem.* **615,** 104 (1992).
6. A. Guesdon, M. M. Borel, A. Grandin, A. Leclaire, and B. Raveau, *J. Solid State Chem.* **108,** 46 (1994).
7. G. Costentin, M. M. Borel, A. Grandin, A. Leclaire, and B. Raveau, *J. Solid State Chem.* **89,** 83 (1990).
8. K. H. Lii, D. C. Johnson, O. P. Goshorn, and R. C. Haushalter, *J. Solid State Chem.* **71,** 131 (1987).
9. C. Gueho, M. M. Borel, A. Grandin, A. Leclaire, and B. Raveau, *J. Solid State Chem.* **104,** 202 (1993).
10. R. C. Haushalter and L. A. Mundi, *Chem. Mater.* **4,** 31 (1992).
11. S. Boudin, A. Grandin, M. M. Borel, A. Leclaire, and B. Raveau, *J. Solid State Chem.* **110,** 43 (1994).
12. S. Boudin, A. Grandin, M. M. Borel, A. Leclaire, and B. Raveau, *J. Solid State Chem.*, in press.
13. A. Benhamada, A. Grandin, M. M. Borel, A. Leclaire and B. Raveau, *J. Solid State Chem.* **104,** 193 (1993).
14. W. H. Zachariasen, *J. Less-Common Metals* **62,** 1 (1978).
15. N. E. Brese and M. O'Keefe, *Acta Crystallogr. Sect. B* **47,** 192 (1991).
16. S. C. Abrahams, L. E. Alexander, T. C. Furnas, W. C. Hamilton, J. Ladell, Y. Okaya, R. A. Young, and A. Zalkin, *Acta Crystallogr.* **22,** 1 (1967).